Supporting Information

Materials and Reagents

Zirconium(IV) butoxide in butanol ($Zr(BuO)_4 \cdot BuOH$, 80% w/w; Sigma Aldrich), dry benzyl alcohol with a molecular sieve (BnOH; analytical grade, Neon), acetone (99.5%, Neon), chloroform (99.9%, Synth), ethanol (99,8%, Neon), and a 3.5 Å molecular sieve (activated at 315 °C for 3 hours; Sigma Aldrich) were used.

Synthesis of Nanocrystals

The synthesis of nanocrystals was carried out using a method widely employed in the literature, with benzyl alcohol as the solvent. Initially, 500 mL of benzyl alcohol was dried with 110 g of molecular sieves for 2 weeks and stored in a dry environment. In a glovebox with a dry atmosphere, 9.4 mL of zirconium butoxide precursor in butanol ($Zr(BuO)_4 \cdot BuOH$) was mixed with 30.6 mL of benzyl alcohol (BnOH) previously dried with a molecular sieve in a glass reaction beaker. The mixture was homogenized and transferred to a sealed stainless-steel reactor, heated by an electric resistance system controlled via PID, and subjected to thermal treatment at 230 °C for 48 h under constant magnetic stirring at 480 RPM. After the reaction, the system was cooled to 50 °C, and the dispersion was separated by centrifugation and washed twice with acetone. The resulting solids were collected and stored in chloroform. For analysis of the solid nanomaterials, the dispersion was dried under a controlled vacuum atmosphere (260 mmHg) at 30 °C.

The same process was conducted with the addition of distilled water to a glass vial previously dried at 110 °C. Deionized water was added to 40 mL of benzyl alcohol previously dried with a molecular sieve at the concentrations indicated in Table 1 for each synthesis. After the water was added, the mixture was homogenized, and the sealed vial was left to rest for at least 12 hours inside the glovebox.

Characterizations

For Raman spectroscopy and X-ray diffraction (XRD) characterization, an aliquot of the dispersion containing the ZrO_2 nanocrystals was withdrawn and dried as described in the methodology. For morphological characterization by X-ray diffraction (XRD), a Shimadzu XRD-6000 diffractometer with Cu-Kα radiation (λ = 0.1541 nm) generated at 40 kV and 30 mA and monochromatized with a nickel filter was used. θ-2θ scans were performed with a scanning speed of $2°\cdot min^{-1}$, an angular step of 0.02°, an acquisition time of 1 second, and a quartz sample holder. Raman spectra were obtained using a Witec alpha 300 confocal Raman microscope with a 20x objective lens, a laser energy of 2.33 eV (λ = 532 nm), and powdered samples deposited on a glass slide. Transmission electron microscopy images were acquired using a Talos F200C (Thermo Fisher Scientific) transmission electron microscope equipped with a field emission electron beam, an accelerating voltage of 200 kV, and a 4k × 4k CMOS camera that enables low-dose acquisitions and side-entry cryogenic sample holders. High-resolution TEM images were also acquired using a Titan Cubens (FEI) with an acceleration voltage of 300 kV and a 4x4k CMOS camera. Automated image acquisition software was used. Coulometric Karl Fischer titration was performed using a Metrohm 756 KF Coulometer equipped with a diaphragm-type generator electrode, and the reagent used was Merck Aquastar® CombiCoulomat fritless. UV–Vis measurements were conducted using a Cary 60 UV–Vis spectrophotometer with a reflectance accessory for solid samples.

The experimental details, calculations, and other applied parameters are applied in the data treatment for each sample.

Water fraction in benzyl alcohol by Karl Fischer coulometry titration: The water fraction is determined in benzyl alcohol solutions by adding the mixture to conditioned Karl Fischer reagent. Additionally, benzyl alcohol was feasible to be measured by the

Aquastar® KF reagent. The experiments were conducted and are listed in Table S 1. Notably, a quick analysis was performed after the container was opened for air exposure, and a thin needle was used to minimize external water contamination. The fitting curve ExpDecay1 **was** applied in the water absorption experiment shown in equation 1.

Table S 1: Water fraction determined by Karl Fischer coulometry and experimental details.

Experiment	Measured water fraction (ppm)	Procedure and experiment details
Dried benzyl alcohol solution with molecular sieves	39	• 500 mL of as-received benzyl alcohol was transferred to a container with 110 g of preactivated 3,5A molecular sieves inside a dried glovebox. • The solution is to rest for over 2 weeks before its use.
Maximum water saturation in benzyl alcohol	90835	• In a closed container, a 50% volume of water and a 50% volume of BnOH. • The mixture was vigorously stirred and left resting for over a week to allow the complete phase separation and guarantee the water saturation in the benzyl alcohol phase. • The water in the BnOH phase was collected by using a needle, cleaning the part exposed to the water phase, and being careful not to take water
Maximum water absorbed from atmospheric air (55~85% relative humidity)	3 weeks: 30535 2nd month: 35050 9th month: 32852 12th month: 35522	• 60 mL of benzyl alcohol in a short-form 100 mL beaker was exposed to atmospheric air for over a year. • In the lab environment in a tropical climate under an air conditioner.
Time versus water absorption in a controlled environment	**Dry (0 min, control 1):** 283 **1 min:** 408 **2 min:** 473 **4 min:** 637 **8 min:** 861 **16 min:** 1281 **32 min:** 1610 **64 min:** 2182 **240 min:** 4033 **Dry (control 1, let sealed in the glove bag for 240 min):** 118 **960 min (16 h):** 6654 **3840 min (64 h):** 9768 **21600 min (360 h):** 33822 **43200 min (720 h):** 41146 **Dry (control 2, let sealed in the glove bag for 720 h):** 1222	• 2 mL of benzyl alcohol was added to an Eppendorf (exposed area is approximately 10 mm^2). The air humidity was measured by the humidity device. • The experiment was conducted inside a glove bag with 3 liters of KCl saturated solution. • The Eppendorfs were opened, and the time to exposure was counted. • They were closed in the given time exposure. • On the second day (after 16 h, concerning the sample 960 min), all Eppendorf tubes were closed to take the first group out from the glovebag (all samples before 960 min and the group control 2). • After that, the second group (over 24 h/1048 min) was taken back to the glovebag and just opened whenever the humidity inside reaches the average condition. • When the experiment finished, over 1 month of exposure, those samples in the second group were characterized together with group control 3.

Size from DRX: Nanocrystal sizes were calculated from DRX data by the well-known Scherrer equation; using the 50,3° peak center, FWHM parameters were calculated from the Pseudo-Voight 1 fitting function, and the shape form was b=0,94 (for spherical and quasispheroidal shapes).

Crystalline phase from DRX: The Rietveld refinements were performed in MAUD software and were compared with the *hkl* reflection positions and relative intensity diffraction for the monoclinic and cubic databases described in ICSD No. 18190 and No. 72955, respectively. The fitting curves and their respective residuals are presented for each sample.

Table S 2: Refined parameters from powder XRD are listed as weight fractions (%), grain size (nm), microstrains (ε), lattice parameters, and statistical Chi² and R-factor for m-ZrO_2 and c-ZrO_2 refinement statistics.

Parameters			Dry	1k	2k	3k	5k	20k	40k
Monoclinic (m-ZrO_2)	Phase composition (%)		83,3 ± 1,7	80,1 ± 1,4	54,4 ± 1,1	48,6 ± 0,7	25,8 ± 1,5	13,0 ± 1,3	44,3 ± 1,2
	Crystallite size (nm)		80,2 ± 1,8	75,6 ± 2,0	66,2 ± 1,3	61,0 ± 1,8	96 ± 14	73,5 ± 20	57,2 ± 1,3
	Microstrain (ε)		0,0146 (4)	0,0108 (6)	0,0092 (3)	0,0092 (6)	0,012 (2)	0,007 (3)	0,0087 (9)
	Lattice parameter (Å)		a = 5,168 (7)	a = 5,151 (6)	a = 5,146 (6)	a = 5,134 (8)	a = 5,15 (2)	a = 5,07 (2)	a = 5,287 (9)
			b = 5,155 (6)	b = 5,172 (5)	b = 5,133 (5)	b = 5,139 (6)	b = 5,20 (2)	b = 5,13 (3)	b = 5,127 (8)
			c = 5,357 (6)	c = 5,335 (4)	c = 5,362 (4)	c = 5,369 (6)	c = 5,27 (2)	c = 5,35 (2)	c = 5,169 (8)
			β= 99,395(7)	β = 99,42 (5)	β = 99,14 (8)	β= 99,16 (9)	β = 99,0 (2)	β = 98,8 (4)	β = 99,4 (1)
Cubic (c-ZrO_2)	Phase composition (%)		16,7 ± 1,5	19,8 ± 0,9	45,6 ± 1,1	51,3 ± 0,4	74,2 ± 1,6	87,0 ± 1,9	55,7 ± 1,3
	Crystallite size (nm)		75 ± 26	64 ± 2,9	58 ± 1,1	65 ± 1,4	53,9 ± 0,3	41,5 ± 0,4	50,162 ± 1,0
	Microstrain (ε)		0,0051 (1)	0,0009 (1)	0,0056 (6)	0,0093 (4)	0,0061 (1)	0,0107 (6)	0,0131 (6)
	Lattice parameter (Å)		a = 5,138 (3)	a = 5,119 (3)	a = 5,114 (1)	a = 5,115 (2)	a = 5,105 (3)	a = 5,115 (3)	a = 5,081 (2)
Statistics	Chi² (ζ)		1,186	1,172	1,155	1,136	1,164	1,115	1,292
	R-factor (%)	R_b	9,519	9,321	9,501	9,102	9,488	8,960	10,001
		R_{exp}	10,363	10,310	10,758	10,562	10,475	10,397	10,143
		R_{wp}	12,287	12,087	12,428	11,997	12,200	11,595	13,113

R_{exp} = expected profile; R_{wp} = weighted profile; R_b = Bragg-R value

Crystalline phase from RAMAN: Due to the given symmetry of each crystalline phase, the group theory allows for the monoclinic, tetragonal, and cubic phases to show 18, 6, and 1 peaks in the RAMAN spectra, respectively. The RAMAN peak is listed for each sample in the tables below, and it is summarized in terms of the peak position and the normalized intensity.

(<10%) VW = Very weak;

(10~30%) W = Weak;

(30~50%) M = Medium;

(50~70%) S = Strong;

(>70%) VS = Very strong;

(Shoulder): This peak appears as a superposed peak, like a shoulder, beside another peak.

Reaction yield: The powders dispersed in chloroform were subjected to thermogravimetry at 700 °C, and the organic ligand fraction was discounted by the yield of the ZrO_2 nanocrystal reaction. The total mass of the ZrO_2 NC dispersion was weighed, and three aliquots of ethanol dispersion were used in the gravimetry calculation.

Optical gap determination (related to the bandgap): From the diffuse UV–Vis spectrograph characterization, the optical gap (bandgap) of the powder samples was calculated from the Tauc plot. This indicates the lowest-energy transition between the valence and conduction band, which was extrapolated from a linear part of the energy equal to zero. Furthermore, the direct allowed transition is considered in the Tauc plots. The percentage of diffuse reflectance for all the samples is presented in Figure S1:

Figure S1: $(\alpha h\nu)^2$ plot from the UV–Vis spectra of powder samples synthesized with different water concentrations.

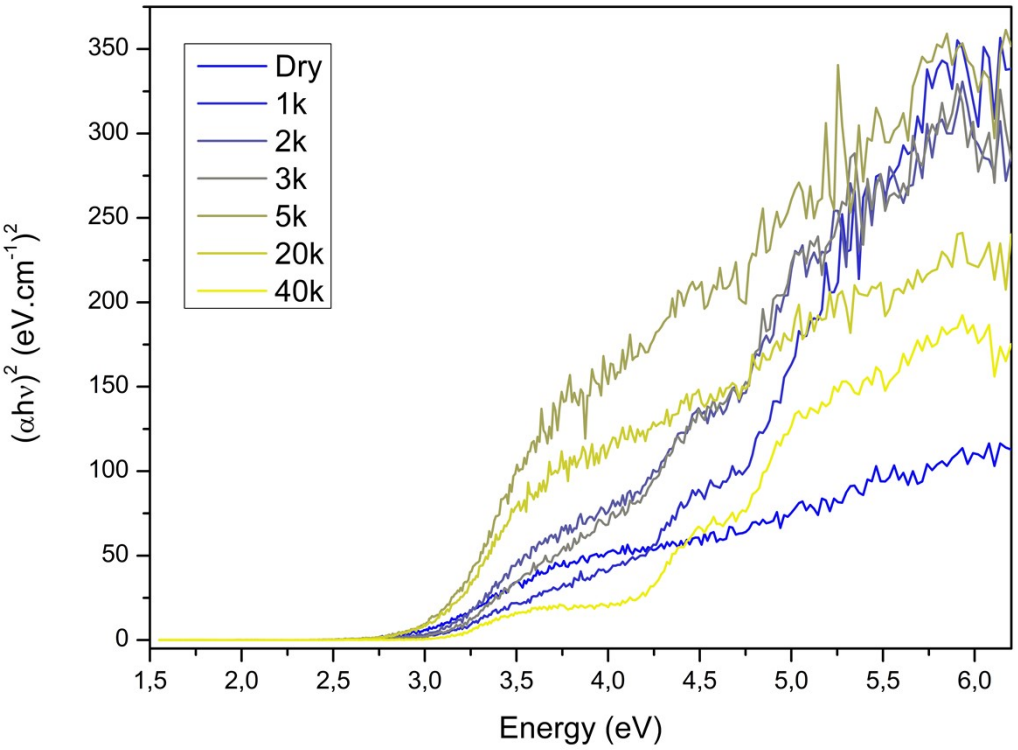

Size and morphology from TEM images: Transmission electron microscopy image is shown for each sample except the 2k and 40k samples. The particle counting was performed using ImageJ software. An ellipsoidal shape was used for all the samples. All the images taken were used for counting the samples.

The kernel smooth distribution curve was applied to estimate the maximum value of the aspect ratio distribution in the bins. [Freq.] = Relative frequency, counts of bins per total count. The peaks of bins in the aspect ratio, the central higher bin plus the vicinal bins, one bin after and one bin below the given center bin (± 1 bin near the center bin).

a) Dry (0k) samples:

Figure S2: Plot of the final number of refinement cycles of the dry (0k) sample.

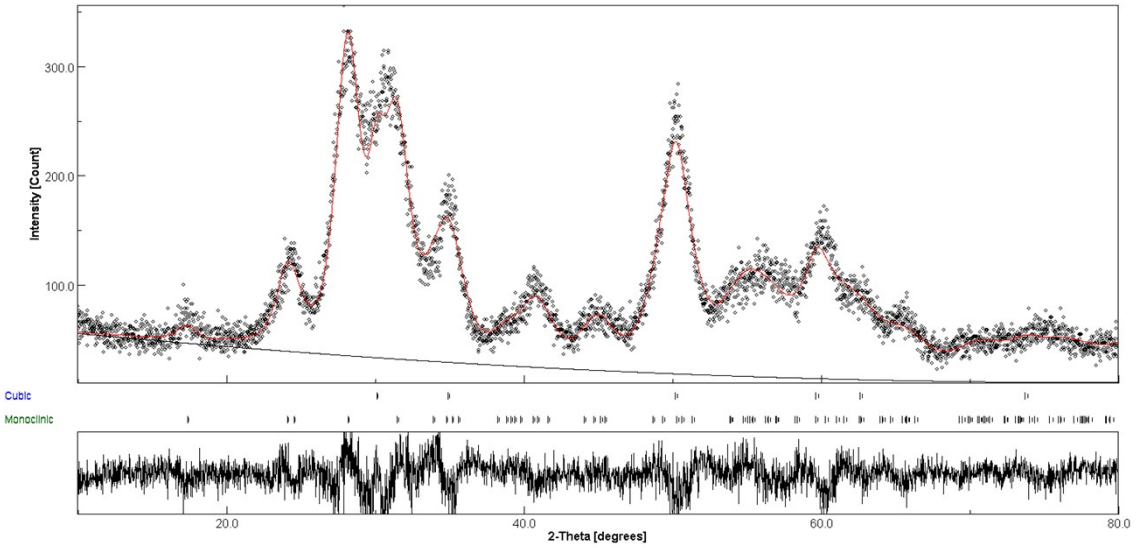

Table S 3: Raman shift peaks of dry (0k) samples and qualitative intensities.

Raman peaks (Dry)	
175 (m/t) – S	**473 (m/t) - VS**
207 (?) – VW	501 (m) – W (Shoulder)
240 (?) – VW	**533 (m) - M**
269 (t) – VW	**556 (m) - M**
307 (m) - VW	**611 (m/c) - VS**
316 (t) – VW (Shoulder)	**642 (t) – M (Shoulder)**
326 (m) - S	669 (?) - W
372 (m) - M	

Figure S 3: Tauc plot method from diffuse reflectance UV–Vis spectroscopy of dry (0k) samples.

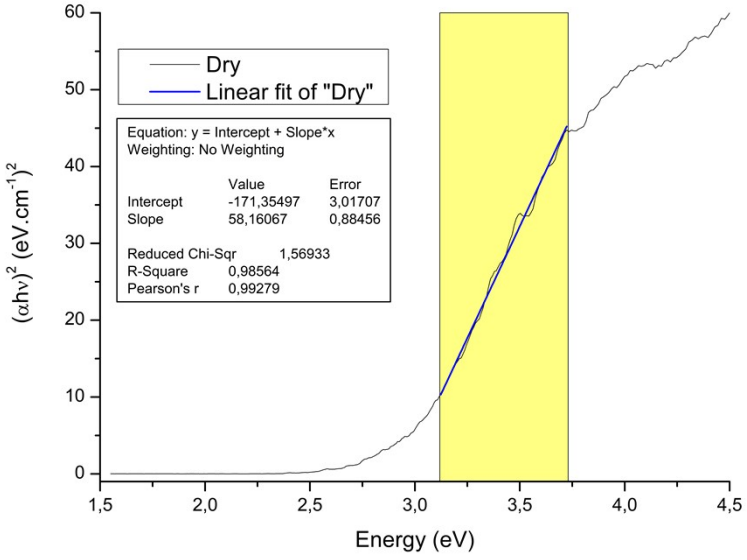

Figure S 4: Transmission electron microscopy images of the dry (0k) sample shown in a) and their respective length and width from 301 total counts b) and with roundness in c).

a)

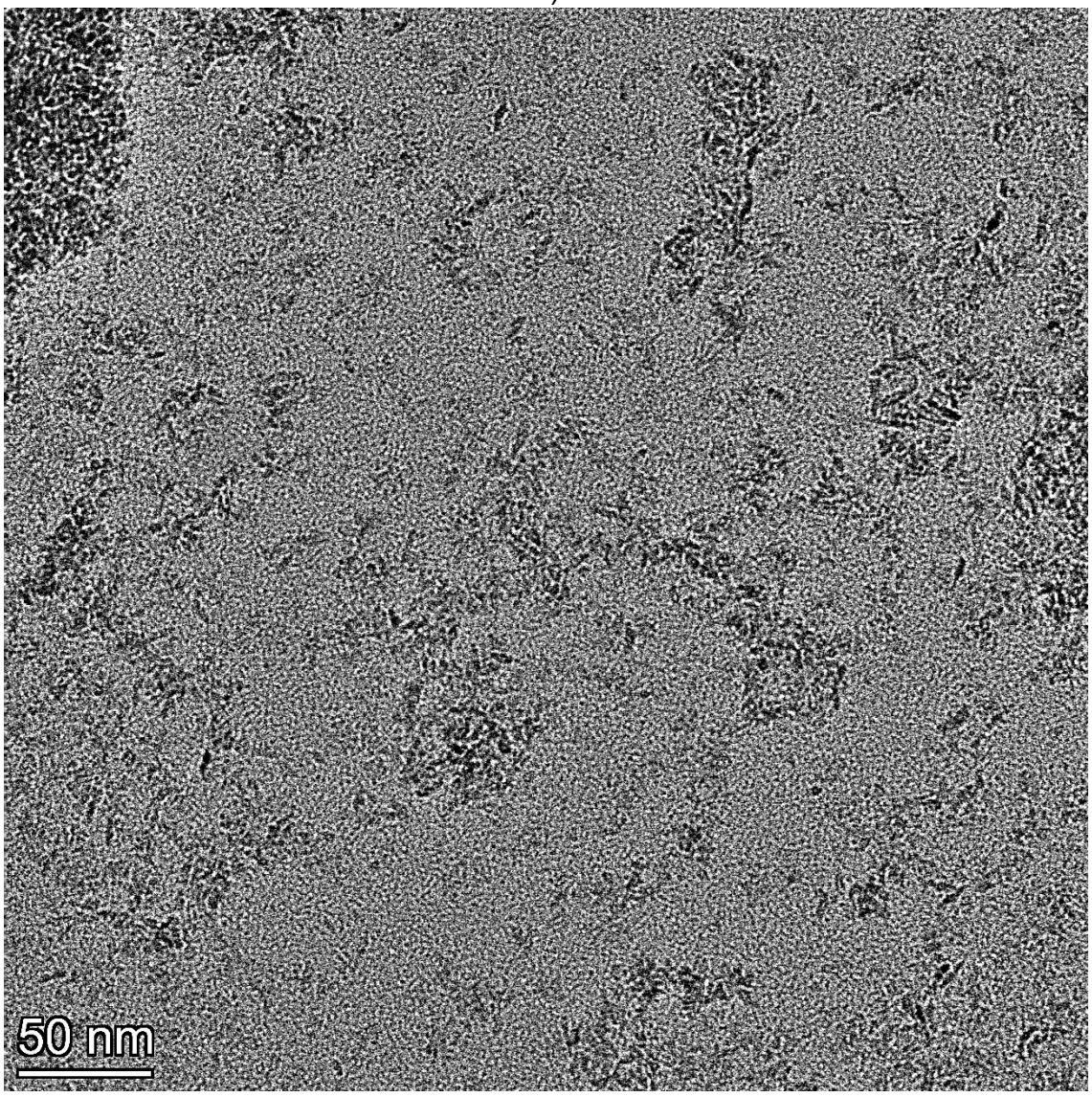

b)

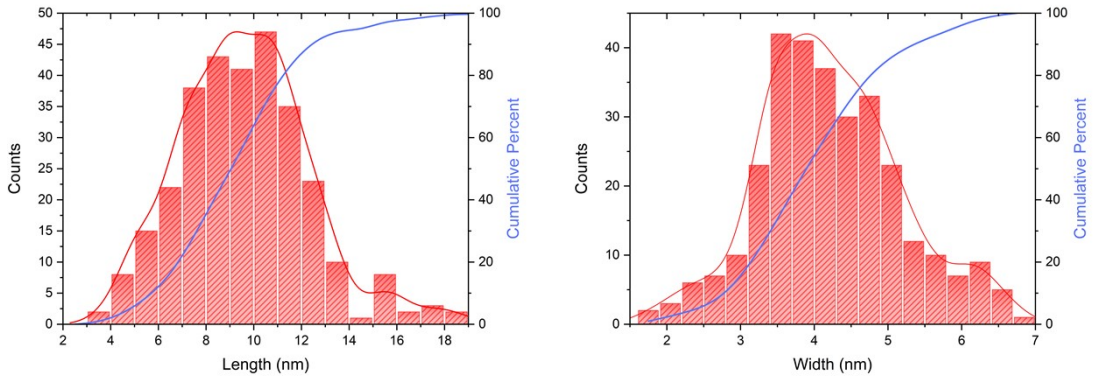

119

120 **c)**

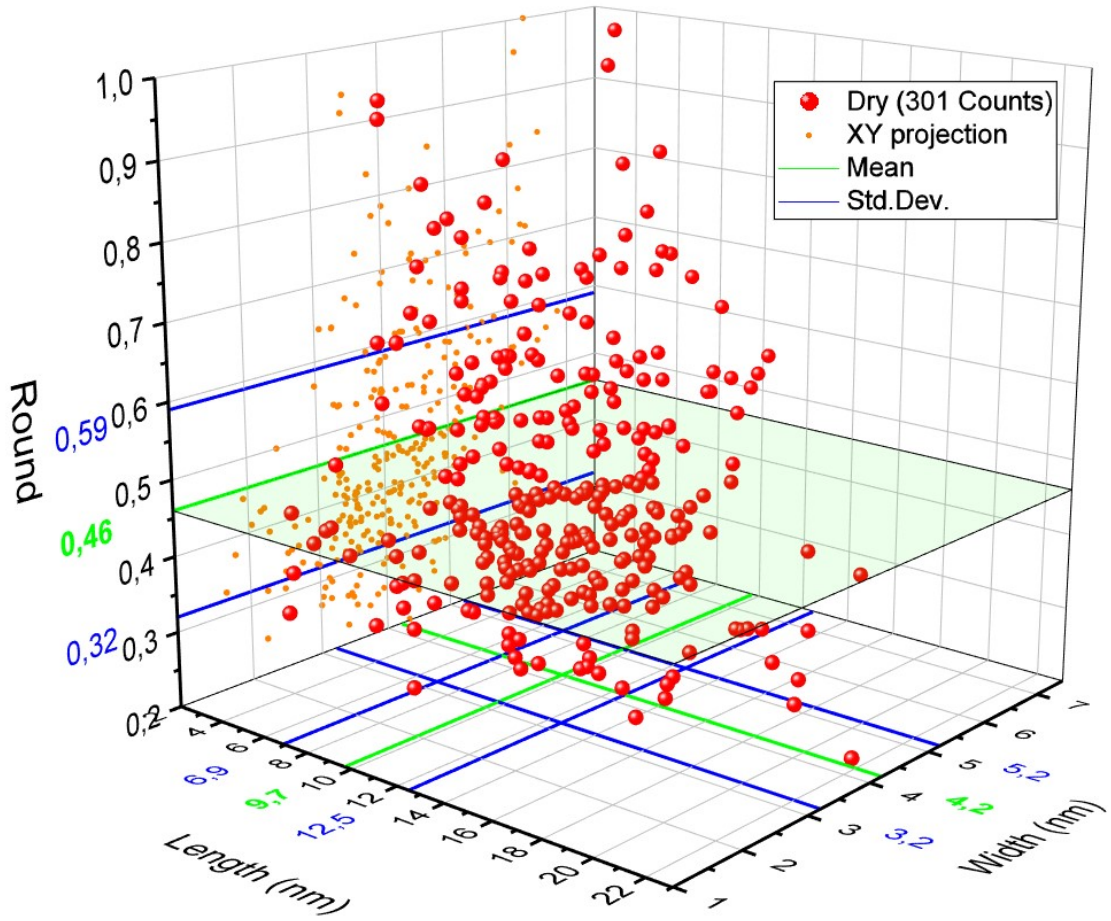

121

122

b) 1,000 ppm (1k) samples

Figure S 5: Plot of the final number of refinement cycles for the 1,000 ppm (1k) sample.

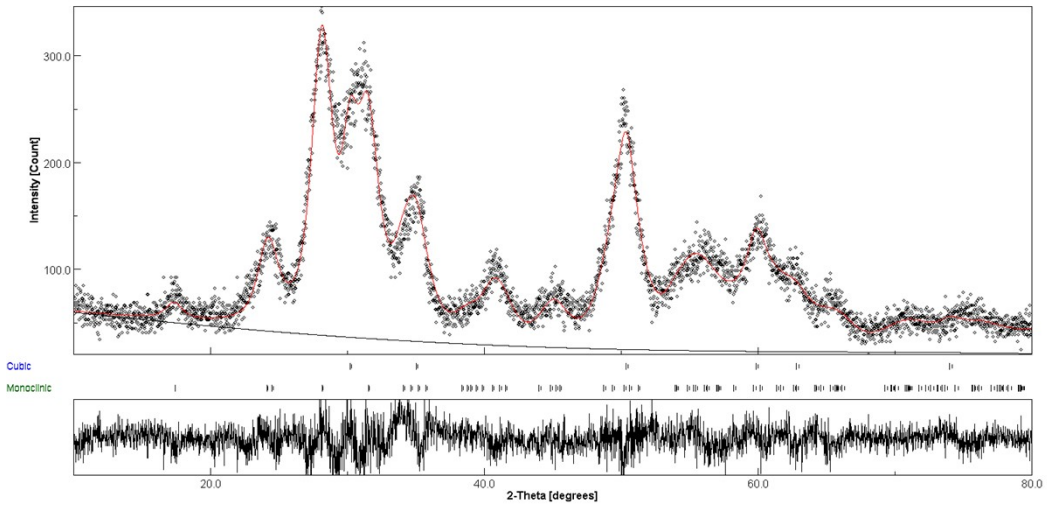

Table S 4: Raman shift peaks of 1,000 ppm (1k) samples and qualitative intensities.

Raman peaks (1k)	
175 (m/t) – S	502 (m) - W
207 (m) - W	**529 (m) – M**
250 (?) – W	**556 (m) - M**
265 (t) - S	570 (t) – W (Shoulder)
302 (m) – M (Shoulder)	**611 (m/c) - VS**
325 (m) - S	**642 (t) - M (Shoulder)**
372 (m) - M	669 (?) - W
473 (m/t) - VS	

Figure S 6: Tauc plot method for the 1,000 ppm (1k) sample obtained by UV–Vis spectroscopy.

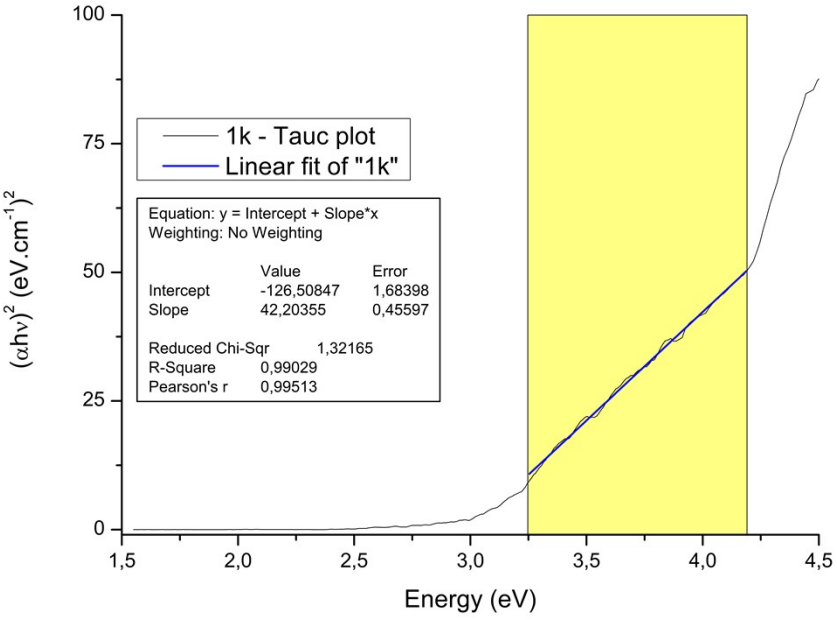

Figure S 7: Transmission electron microscopy images of the 1k sample shown in a) and their respective length and width from 63 total counts b).

a)

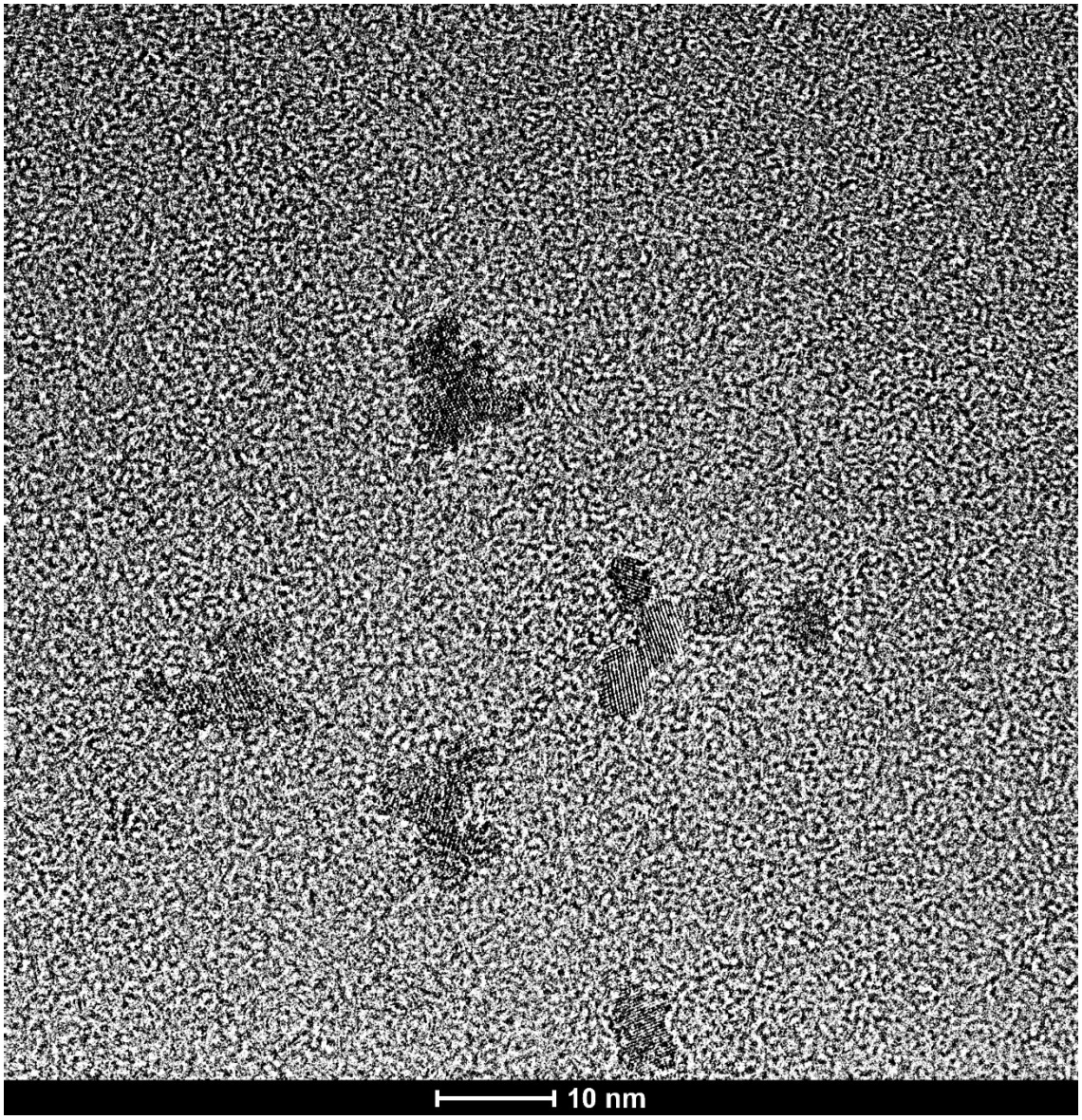

b)

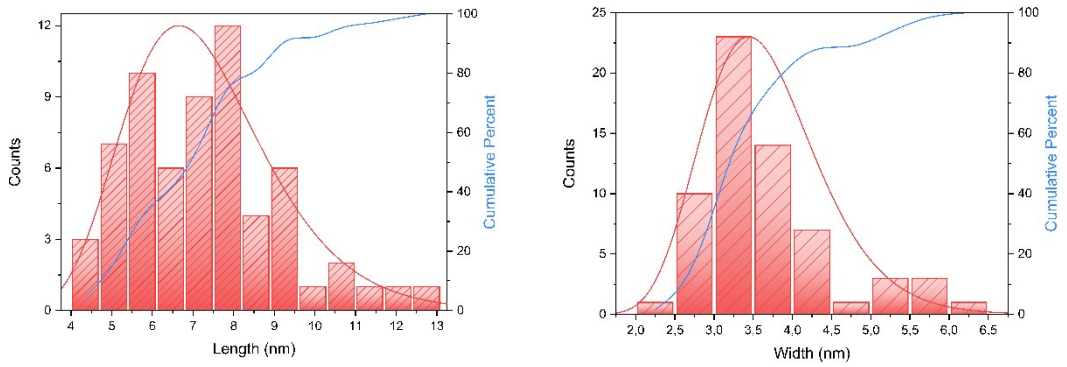

c) 2,000 ppm (2k) samples:

Figure S 8: Plot of the final refinement cycles of the 2,000 ppm (2k) sample.

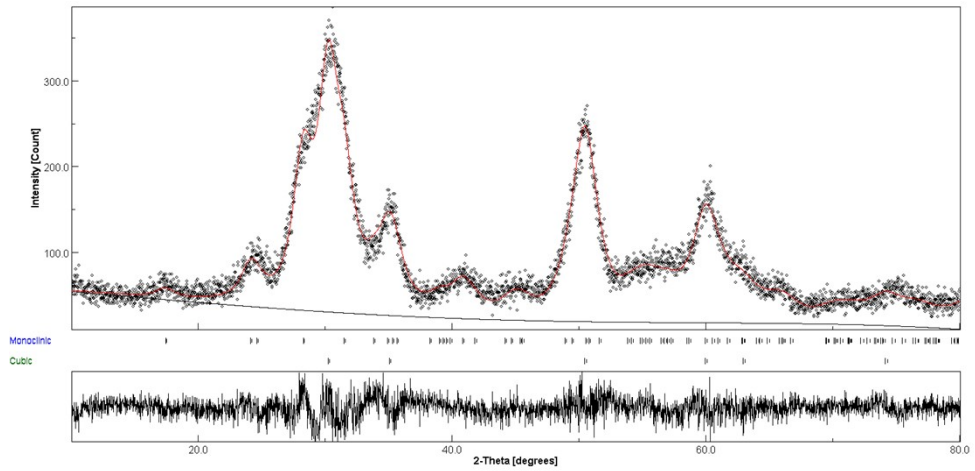

Table S 5: Raman shift peaks of 2,000 ppm (2k) samples and qualitative intensities.

Raman peaks (2k)	
175 (m/t) – S	**473 (m/t) – VS**
208 (m) - VW	496 (m) - W
245 (?) – W	**528 (m) - M**
269 (t) – W	**561 (m) – M**
302 (m) – S (Shoulder)	588 (t) – W (Sholder)
316 (t) - VS	**611 (m/c) - VS**
372 (m) – M	**642 (t) – S (Sholder)**
400 (?) – VW	669 (?) - W
450 (t) – W (Sholder)	

Figure S 9: Tauc plot method from UV–Vis spectroscopy of a 2,000 ppm (2k) sample.

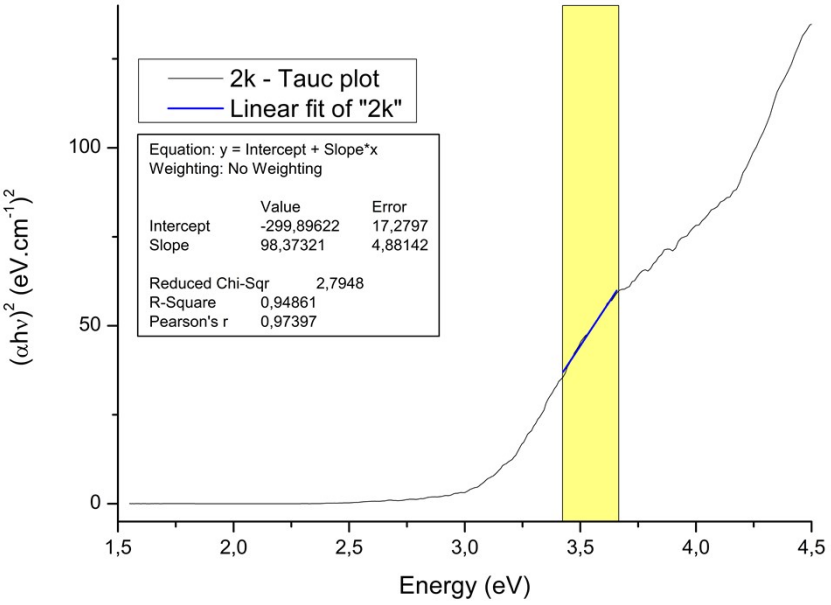

d) 3,000 ppm (3k) sample:

Figure S 10: Plot of final refinement cycles of the 3,000 ppm (3k) sample.

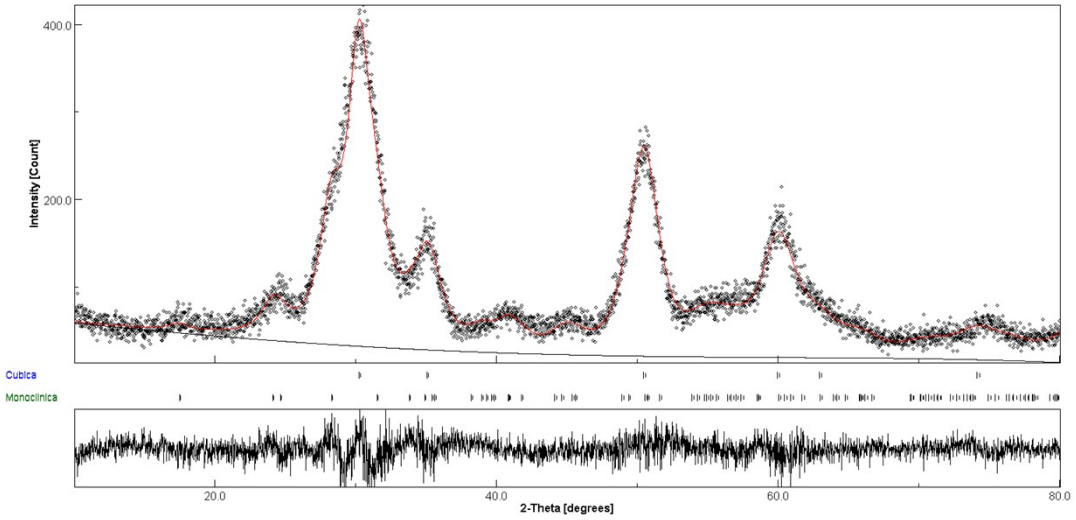

Table S 6: Raman shift peaks of 3,000 ppm (3k) samples and qualitative intensities.

Raman peaks (3k)	
175 (m/t) – S	**473 (m/t) – VS**
207 (m?) - W	**502 (m) – M (Shoulder)**
246 (?) – W (Shoulder)	**528 (m) – M**
265 (t) – W	**561 (m) - M**
302 (m) – M	**570 (t) – M (Shoulder)**
316 (t)	**611 (m/c) - VS**
372 (m) – W	**642 (t) – S (Shoulder)**
404 (?) - VW	669 (?) – W (Shoulder)
450 (t) – W (Shoulder)	

Figure S 11: Tauc plot method from UV–Vis spectroscopy of a 3,000 ppm (3k) sample.

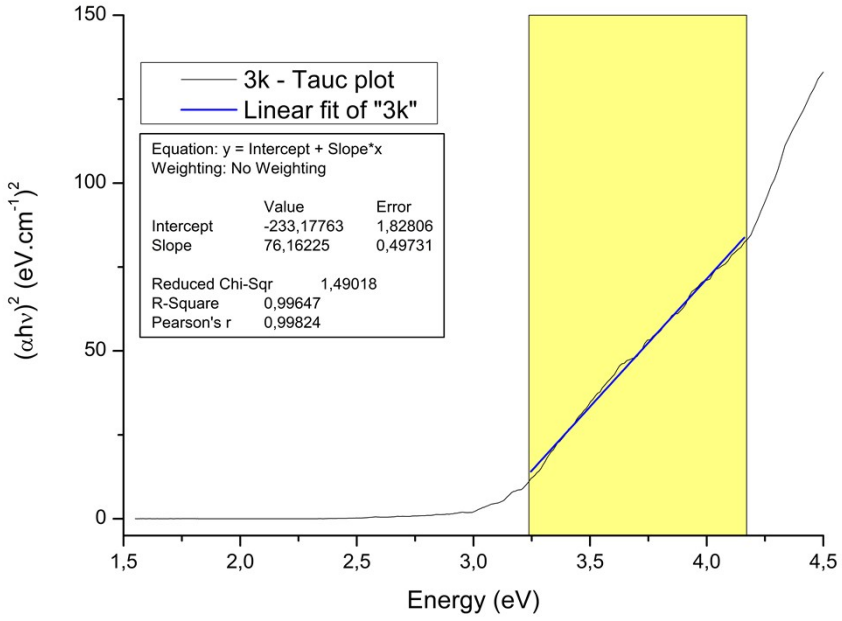

Figure S 12: Transmission electron microscopy images shown in a) and their respective lengths and widths from 160 total counts b).

a)

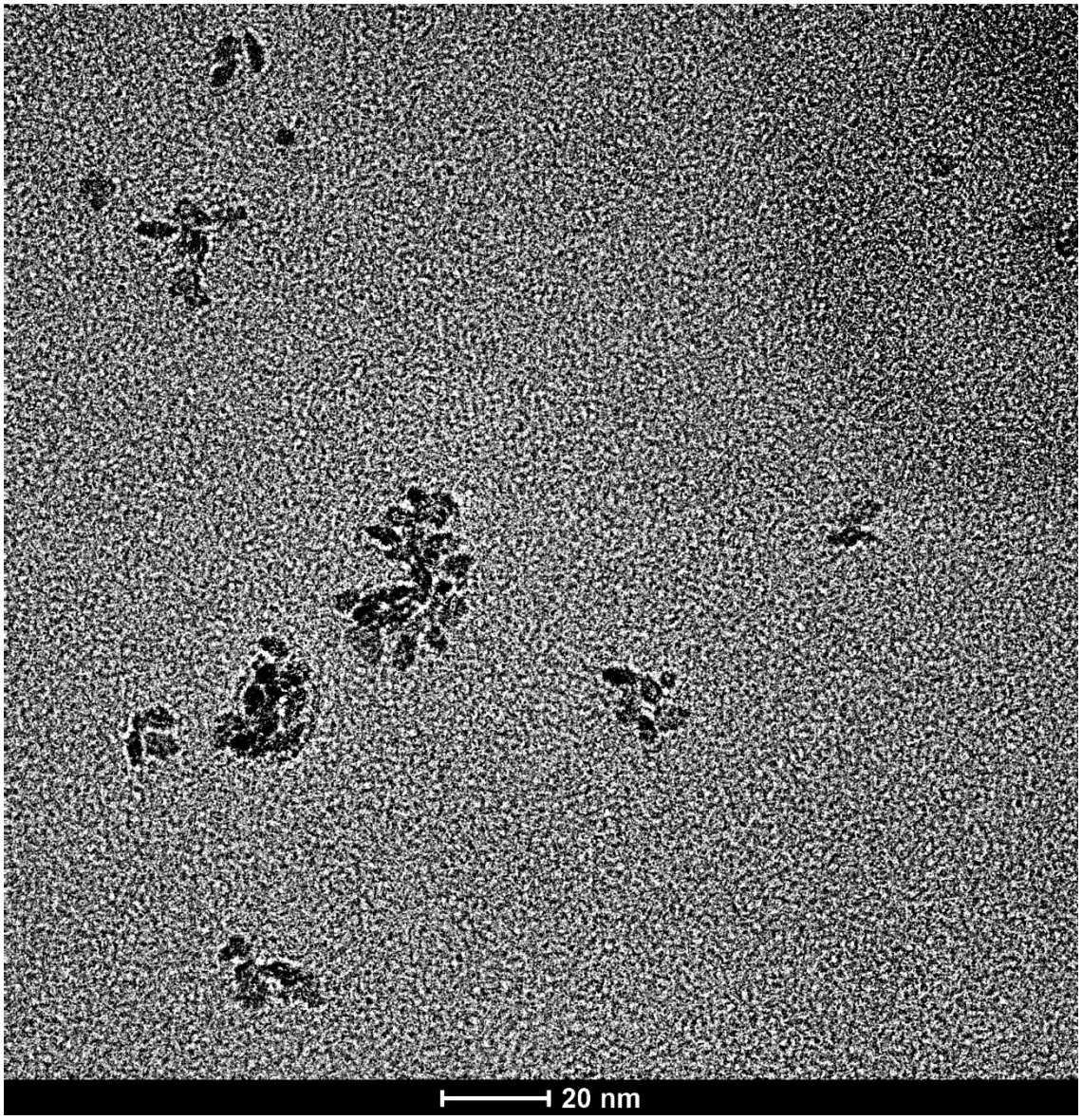

b)

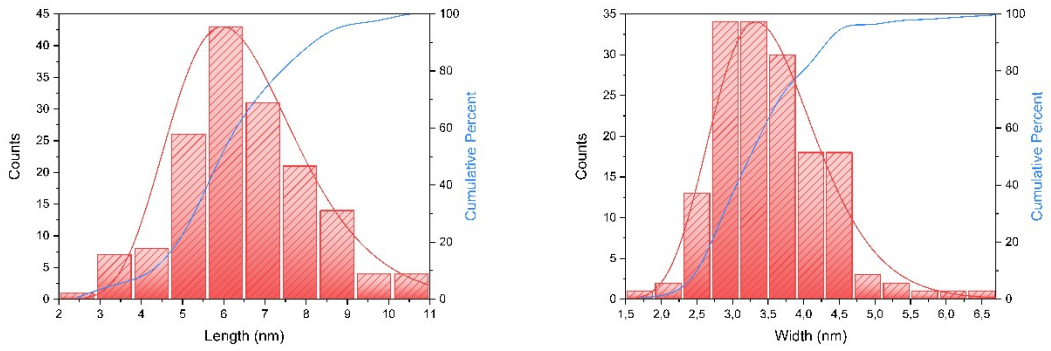

e) 5,000 (5k) sample:

Figure S 13: Plot of the final refinement cycles of the 5,000 ppm (5k) sample.

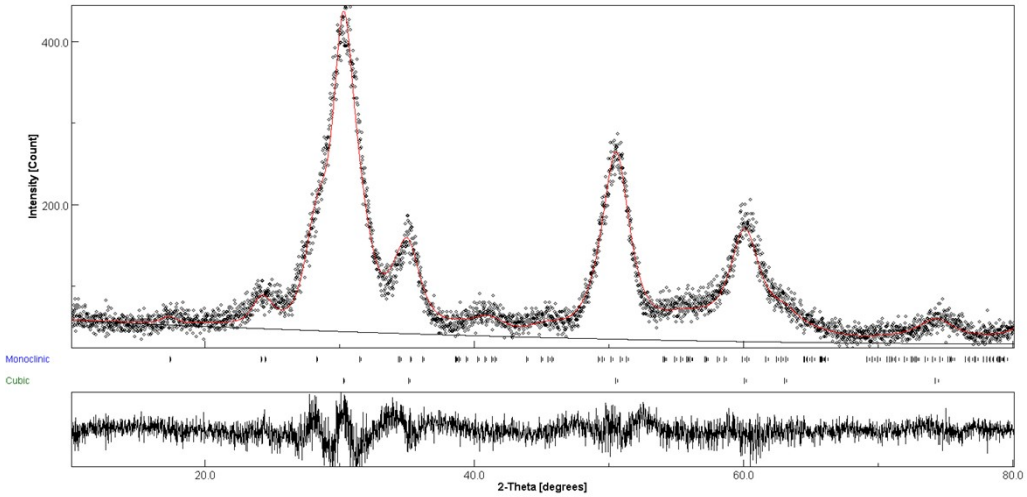

Table S7: Raman shift peaks of 5,000 ppm (5k) samples and qualitative intensities.

Raman peaks (5k)	
179 (m/t) – S	501 (m) – VW (Shoulder)
278 (t) – M	533 (m) - W
320 (t) -S	556 (m) – W
376 (m) - W	**579 (t) – S (Shoulder)**
404 (m) - VW	**615 (m/c) – VS**
473 (m/t) – VS	**642 (t) – VS (Shoulder)**

Figure S 14: Tauc plot method from UV–Vis spectroscopy of a 5,000 ppm (5k) sample.

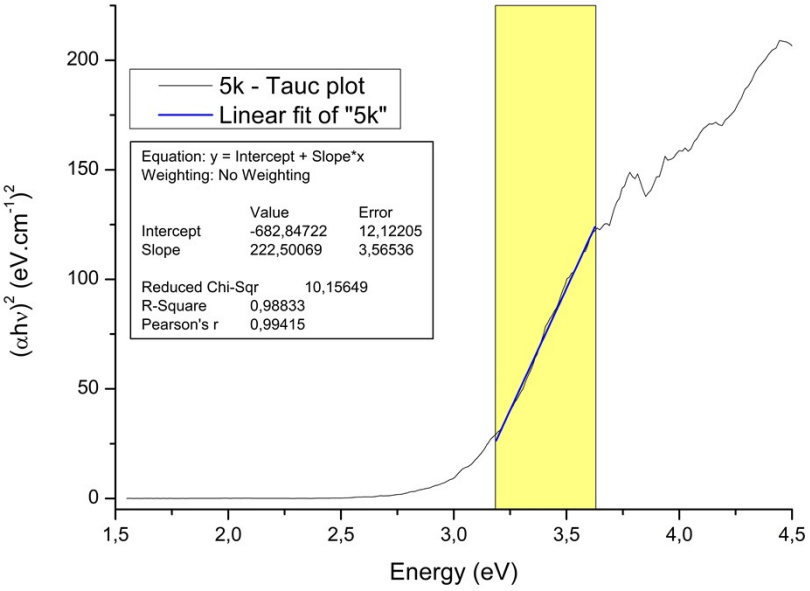

Figure S 15: Transmission electron microscopy images shown in a), and their respective lengths and widths from 301 total counts in b) and with roundness in c)

a)

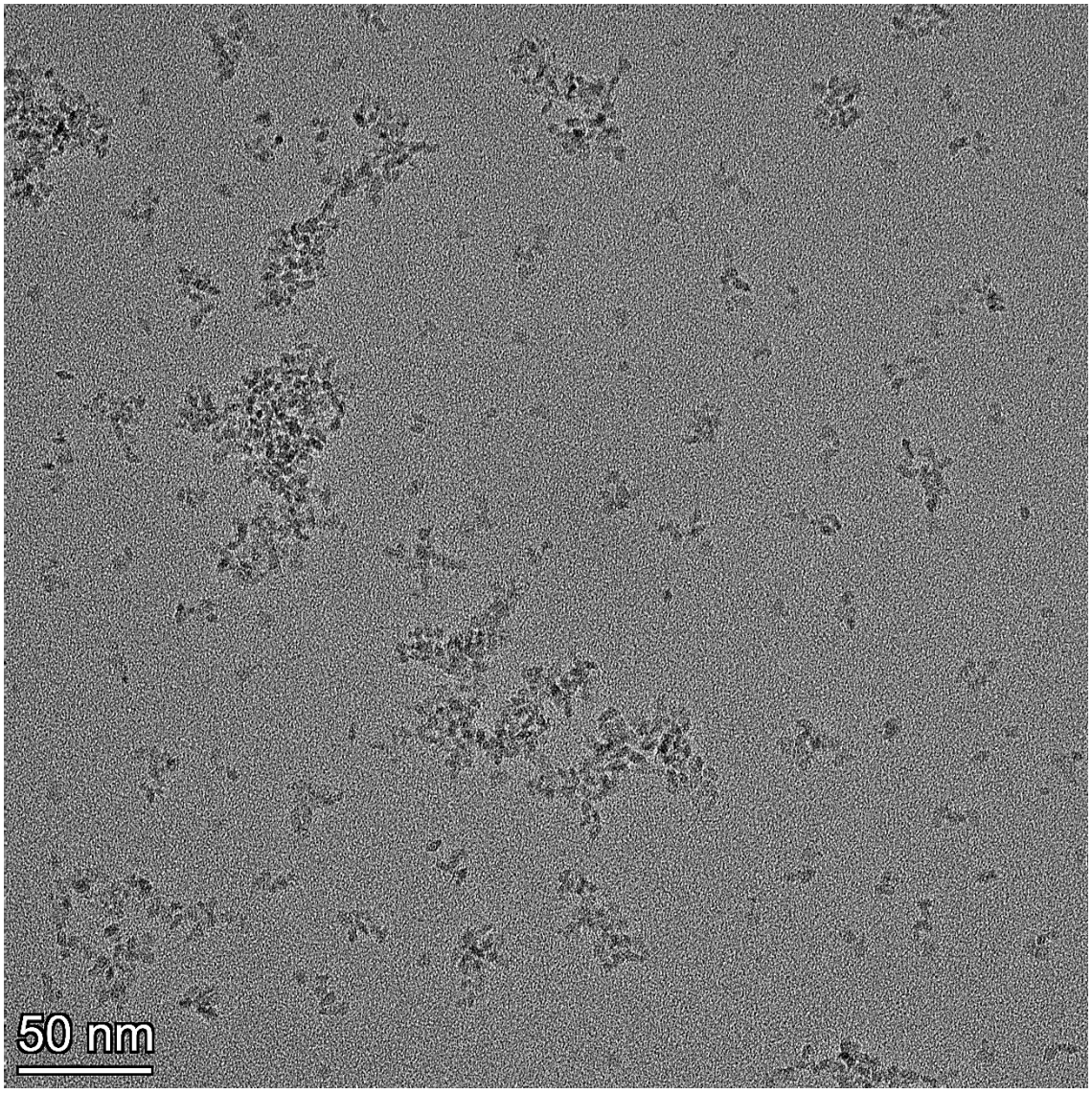

b)

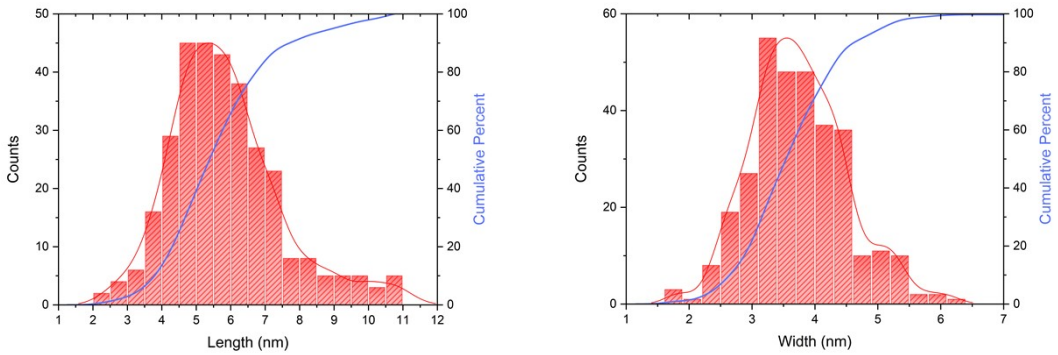

167

c)

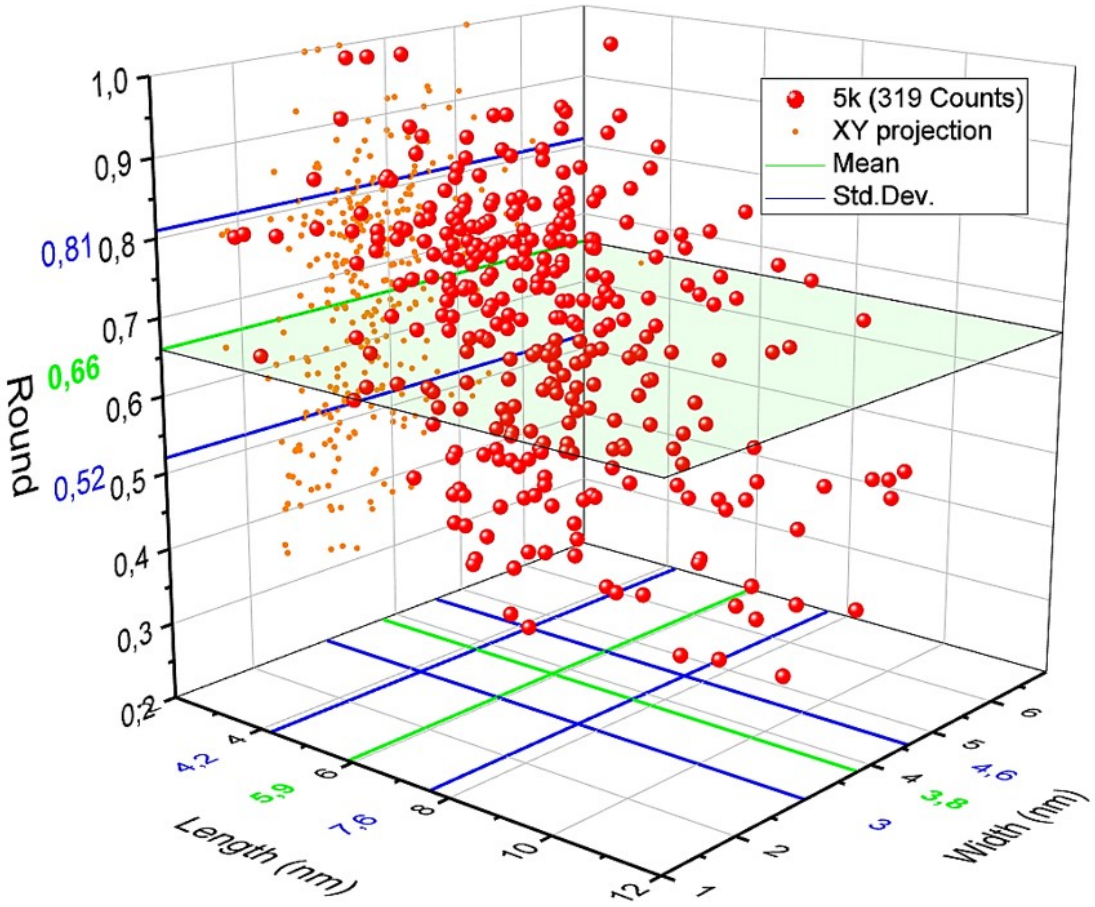

168

169

170

f) 20,000 ppm (20k) sample:

Figure S 16: Plot of final refinement cycles of the 20,000 ppm (20k) sample.

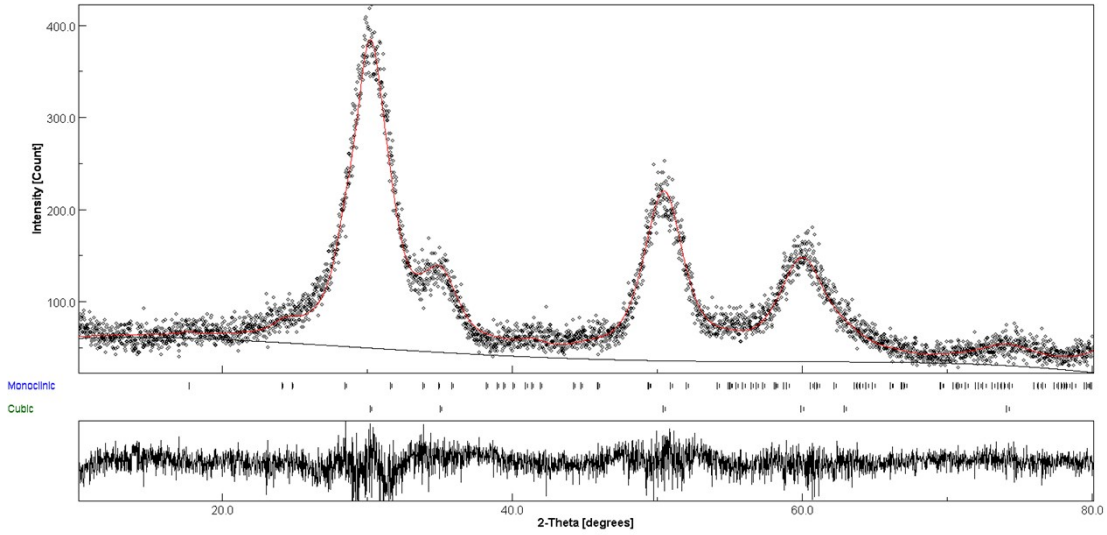

Table S 7: Raman shift peaks of 20,000 ppm (20k) samples and qualitative intensities.

Raman peaks (20k)	
169 (m/t) – M	450 (t) – W (Shoulder)
246 (?)	**473 (m/t) - M**
265 (t) – W	502 (m) - W
302 (m) – W	533 (m) – W (Shoulder)
325 (?) – W (Shoulder)	561 (m) - W
372 (m) – VW	**611 (m/c) - VS**
395 (m) – VW	642 (m/t) – W (Shoulder)
437 (?) – VW (Shoulder)	669 (?) – W (Shoulder)

Figure S 17: Tauc plot method from UV–Vis spectroscopy of a sample at 20,000 ppm (20k).

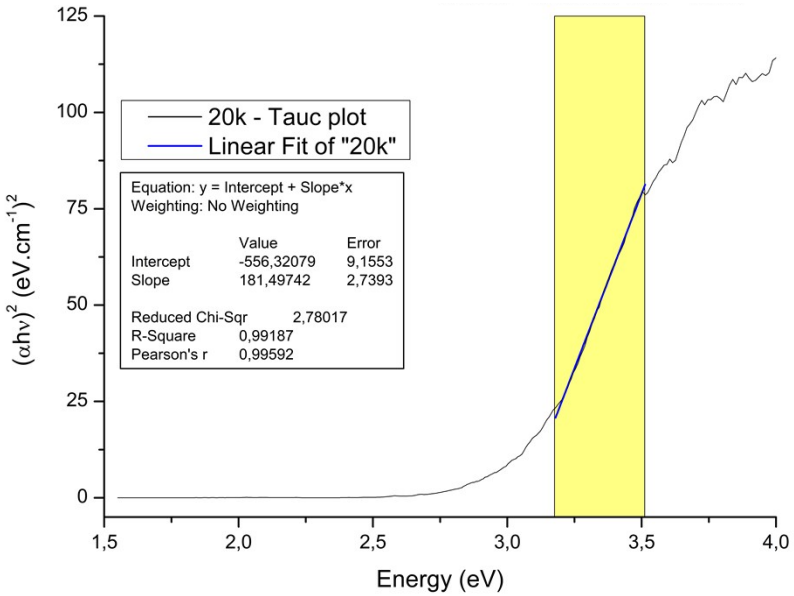

Figure S 18: Transmission electron microscopy images shown in a) and their respective lengths and widths from 408 total counts b) and with roundness in c).

a)

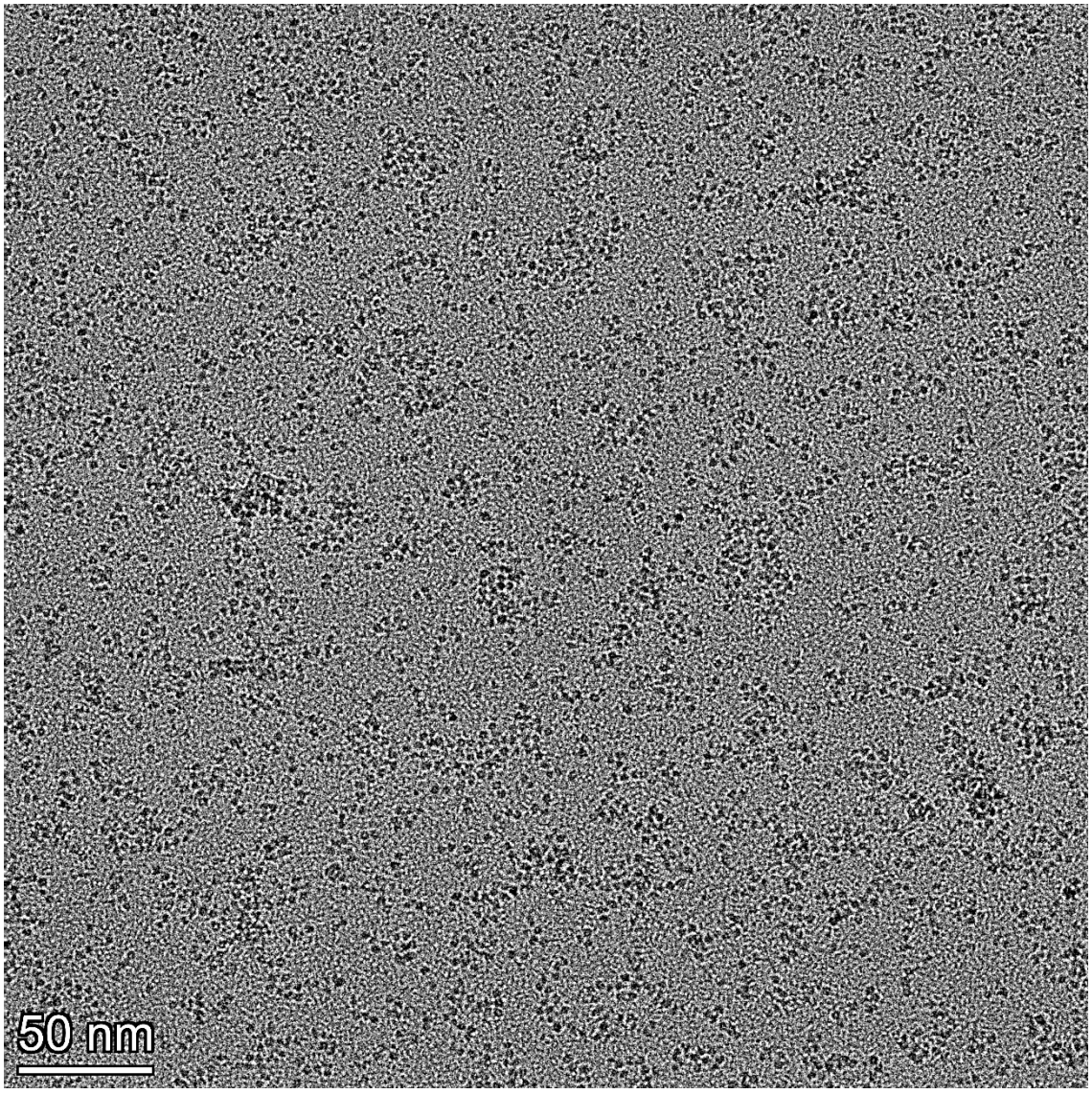

b)

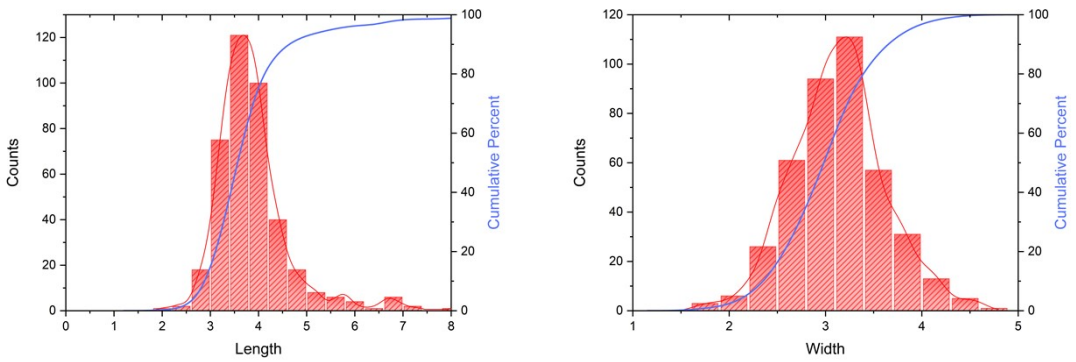

186 **c)**

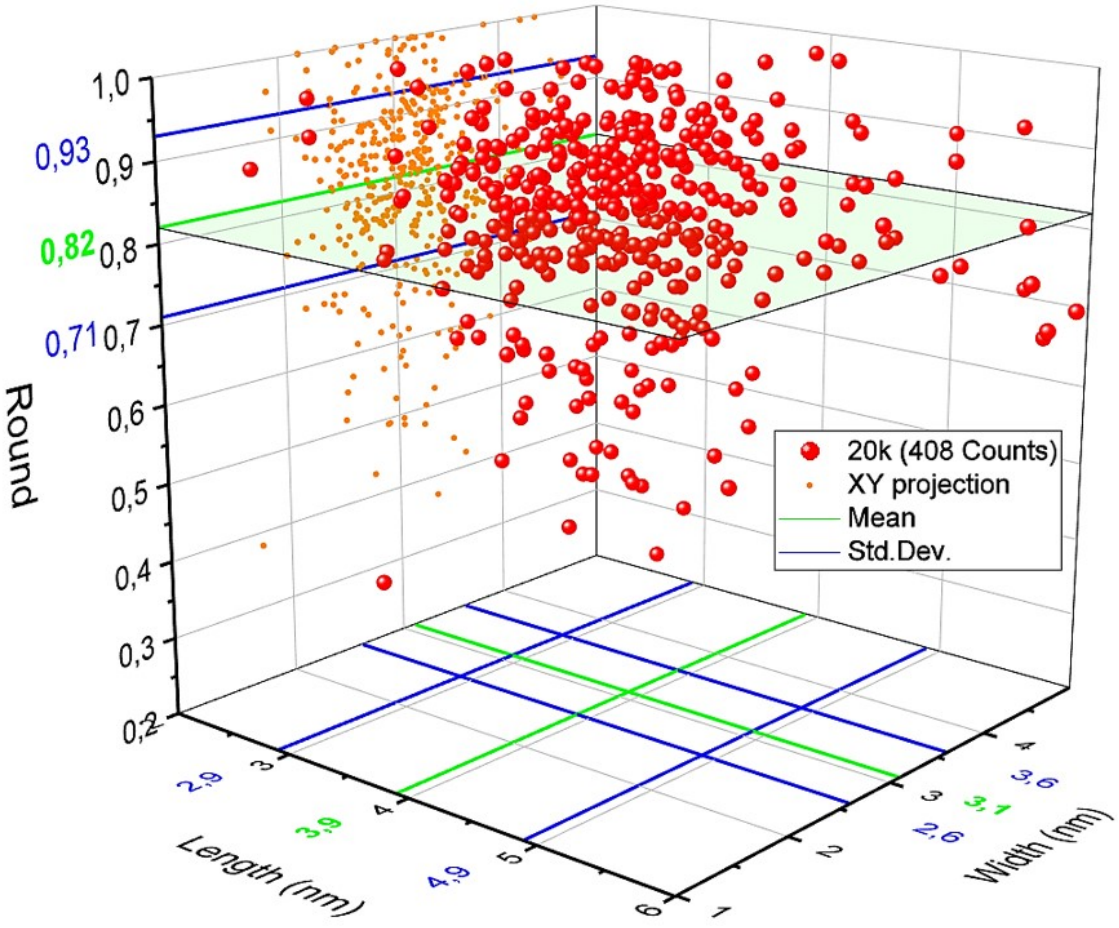
Round
1,0
0,9
0,8
0,7
0,6
0,5
0,4
0,3
0,2
0,93
0,82
0,71
20k (408 Counts)
XY projection
Mean
Std.Dev.
Length (nm)
2,9
3,9
4,9
Width (nm)
2,6
3,1
3,6

187

188

g) 40,000 ppm (40k) sample:

Figure S 19: Plot of the final number of refinement cycles for the 40,000 ppm (40k) sample.

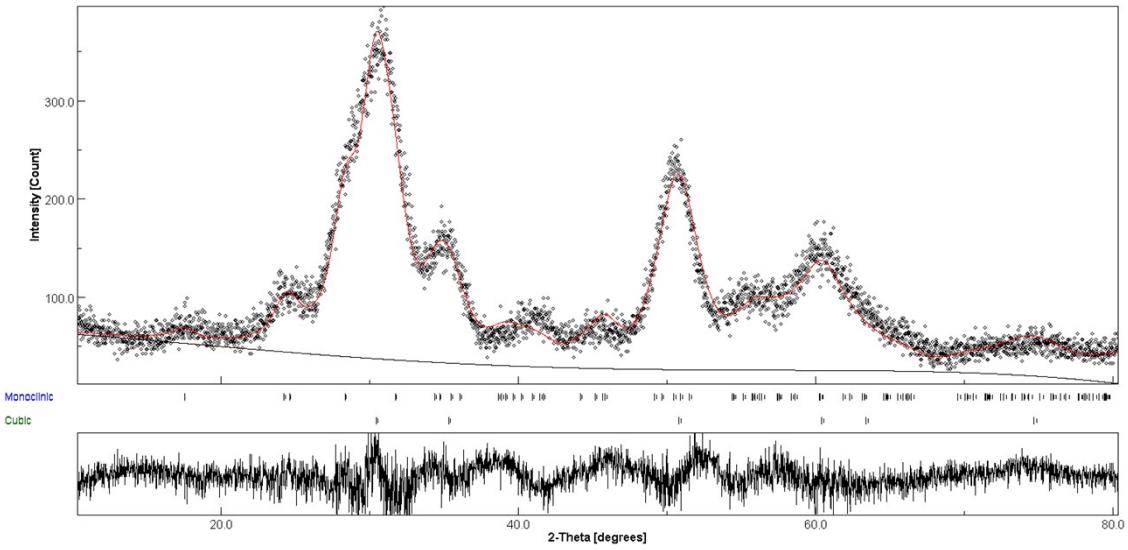

Table S 8: Raman shift peaks of 40,000 ppm (40k) samples and qualitative intensities.

Raman peaks (40k)	
175 (m/t) - S	400 (?) – W (Shoulder)
203 (m?) – VW (Shoulder)	455 (t) – W (Shoulder)
246 (?) – VW (Shoulder)	**473 (m/t) – S**
265 (t) - M	528 (m) – W
302 (m) – W (Shoulder)	561 (m) - W
316 (t) - M	**611 (m/c) - VS**
372 (m) - M	642 (t) – W (Shoulder)

Figure S 20: Tauc plot method from UV–Vis spectroscopy of the 40,000 ppm (40k) sample.